INFN/AE - 67/5
15 Maggio 1967

PROPOSAL TO MEASURE THE PHASE OF THE PION-NUCLEON SCATTERING AMPLITUDE AT VARIOUS ENERGIES AND AT NON-ZERO MOMENTUM TRANSFER

L. Bertocchi*), F. Bradamante†), G. Fidecaro*†),
M. Fidecaro*), M. Giorgi†), F. Sauli†) and P. Schiavon†).

15 May 1967

---

*) CERN, Geneva, Switzerland.

†) Istituto di Fisica della Università, Trieste, and Istituto Nazionale di Fisica Nucleare, Sezione di Trieste, Italy.

/755/5
hsi/p

Summary

A study of the differential cross-section of pion-deuteron elastic scattering should provide information on the phase of the pion-nucleon scattering amplitude at non-zero momentum transfer, taking advantage of the interference between single and double scattering.

An experimental set-up is here proposed, consisting of scintillation counters and wire spark chambers with magnetostrictive read-out, which combines a large angular acceptance and a good accuracy in the determination of the momentum transfer.

67/755/5
hsi/p

1. INTRODUCTION

The aim of the experiment is to measure the phase of the pion-nucleon scattering amplitude at high energies and non-zero momentum transfer; more precisely, to measure the ratio of the real to the imaginary part of the symmetric πp scattering amplitude

$$T^{(+)} = \frac{1}{2}\left[T_{\pi^+ p} + T_{\pi^- p}\right]$$

at a momentum transfer of the order of $|t| = 0.35\ (\mathrm{GeV}/c)^2$, by the measurement of a dip in the elastic pion-deuteron angular distribution at this value of t.

This method has first been proposed by Franco[1], in the framework of a general method discussed by Glauber and Franco[2], and then applied to the elastic pd scattering at 2 GeV incident energy[3] by Coleman and Franco[4], and to the elastic p-^{4}He scattering[5] by Czyz and Lesniak, and Bassel and Wilkin[6].

The physical basis of the method is as follows. In the high-energy region, the pion-deuteron scattering amplitude is expressed, in the Glauber theory, as a sum of terms in an impulse series, whose main terms at small momentum transfer are the single scattering term and the double scattering term. In the Glauber approximation (impact parameter approximation for the pion-nucleon scattering), high energy has the following meaning:

7/755/5
hsi/p

i) the wavelength of the incident particle is smaller than the deuteron size;

ii) the elementary pion-nucleon elastic cross-section has to be concentrated mainly in a forward peak, whose corresponding "optical radius" has also to be smaller than the deuteron size.

These conditions are satisfied in the pion-deuteron scattering when the energy of the incident pion is larger than, say, 800 MeV. In fact, at the corresponding energy, the pion-nucleon scattering amplitude already shows a forward "diffraction" peak.

The small momentum transfer condition is given by the necessity, in the Glauber approximation, of neglecting the effects of the recoil of the deuteron; however, this condition can be relaxed if the Glauber theory is reobtained starting from a Feynman diagram approach[7], which allows one to take care of the recoil and relativity corrections; in this way the theory can be expected to be valid in a range of momentum transfer

$$0 \leq |t| \lesssim 1 \ (\mathrm{GeV}/c)^2 .$$

In the Glauber theory, the pion-deuteron scattering amplitude is given by

$$F(\vec{q}) = f_n(\vec{q})G\left(\frac{\vec{q}}{2}\right) + f_p(\vec{q})G\left(-\frac{\vec{q}}{2}\right) + \frac{i}{2\pi k}\int d_2\vec{q}'\, G(\vec{q}) f_n\left(\frac{\vec{q}}{2} + \vec{q}'\right) f_p\left(\frac{\vec{q}}{2} - \vec{q}'\right) \qquad (1)$$

where $f_p(\vec{q})$ and $f_n(\vec{q})$ are the pion-proton and pion-neutron scattering amplitudes, $G(\vec{q})$ is the deuteron form factor, which can be expressed as the Fourier transform of the square of the deuteron bound state wave function

$$G(\vec{q}) = \int d^3x \ |\psi(x)|^2 \ e^{i\vec{q}\cdot\vec{x}} .$$

The variables are such that $\vec{q}$ is the momentum transfer vector ($\vec{q}^2 = -t$ in the Breit system), and, if $\vec{k}$ is the momentum of the incident pion in the lab system, $\vec{q}'$ is a two-dimensional vector, orthogonal to $\vec{k}$. The first two terms correspond to single scattering, where the pion interacts with only the proton (or the neutron) inside the deuteron; the third term is the double scattering term, where the pion interacts with both nucleons.

At high energy, where the pion-nucleon scattering shows a forward peak, the single and double scattering term have a completely different behaviour with the momentum transfer.

Firstly, in the forward direction, the single scattering terms are much more important than the double scattering term; it is known that at $t = 0$, applying the optical theorem, the first two terms express the πd total cross-section as the sum of the πp and πn total cross-section, and the third gives rise to the Glauber shadow correction, proportional to the product of the πp and πn total cross-section, which turns out to be a few per cent correction.

At non-zero angle, the single scattering term decreases very fast with t, while the double scattering term has a much more gentle slope. A way of estimating the slopes is to take both the deuteron form factor and the pion nucleon scattering amplitudes as exponentials in t: $G(-t/4) = e^{b_1 t}$, $f(t) = f(0)\, e^{bt}$. Then the values of b and b_1 can be taken as $b_1 \simeq 8$ $(\mathrm{GeV/c})^{-2}$, $b \simeq 4$ $(\mathrm{GeV/c})^{-2}$. With this parametrization, the single and double scattering amplitudes have the behaviour with t

$$T_{single}(t) = T_s(0)\, e^{b_s t} ; \quad T_{double}(t) = T_d(0)\, e^{b_d t} ,$$

with $b_s = 12$ $(\mathrm{GeV/c})^{-2}$, $b_d = 2$ $(\mathrm{GeV/c})^{-2}$. The fact that $T_s(0) \gg T_d(0)$ means that for some value of t, $t = t_0$, the absolute values of T_{single} and T_{double} coincide. If the deuteron form factor is properly computed from a deuteron wave function which reproduces well the rapid decrease of the elastic cross-section at small t, and including the proper amount of D-wave function, the value of t_0 can be estimated to be of the order of $t_0 \simeq -0.35$ $(\mathrm{GeV/c})^2$.

67/755/5
hsi/p

If the pion-nucleon scattering amplitudes are supposed to be purely imaginary, with positive imaginary part, for all values of t, then it is easy to see from formula (1) that the single and double scattering amplitudes are both purely imaginary and of the opposite sign. The two contributions therefore tend to cancel.

As a result the elastic pion-deuteron angular distribution will show a zero for $t = t_0$. In general, if the real part of the pion-nucleon scattering amplitude is non-zero, instead of a zero the angular distribution will show a dip; this dip is filled up very rapidly when the real part is increased from zero. Therefore, the form of the elastic differential cross-section of the pion-deuteron scattering is very sensitive to the real part of the pion-nucleon scattering amplitude at a value of t close to t_0. One has to stress that at high energies, where no phase-shift analysis is possible due to the large number of angular momenta involved, there is actually no way of measuring experimentally the phase of a scattering amplitude, except at t = 0, where one can obtain the real part from the Coulomb interference experiments. The fact that the deuteron has isospin zero has the result that the relevant real part is that of the symmetric pion-nucleon amplitude *).

The reason for choosing a pion-deuteron scattering instead of proton-deuteron (where one could have much more intense beams), is that the theoretical analysis is far easier when the elementary interaction is the pion-nucleon scattering amplitude, which depends only on two invariant amplitudes in the spin space, in contrast with the nucleon-nucleon amplitude, which depends on five invariant amplitudes.

We think that it is important to perform two kinds of experiments, one at rather moderate energies (typically below 1 GeV), the second one at high energies (starting for example at 6 GeV).

---

*) The symmetric amplitude is the only one which is present in the single scattering term. The double scattering contains also the square of the antisymmetric contribution; however this effect, being a quadratic one, is small at high energies.

67/755/5
hsi/p

The aim of the intermediate energy experiment is twofold. First of all, it is an energy at which one can still have a good knowledge of the pion-nucleon scattering amplitude, obtained from the elastic scattering and polarization measurements for $\pi^{\pm}p$ scattering. One can therefore, using the existing knowledge of the deuteron wave function, predict the actual position, width and deepness of the dip at $t = t_0$; the measurement will in this way be a check of the Glauber theory. In this connection, it would be useful to perform also an accurate measurement, at the same energies, of the elastic $\pi^{\pm}p$ angular distribution, which will also have a separate interest for the phase-shift analysis of pion-nucleon scattering*). On the other hand, the deuteron parameters are not so well known in the relevant interval of momentum transfer; a recent analysis by the Gourdin group of the elastic electron-deuteron scattering and of the deuteron photo- and electro-disintegration[8] shows that one has some knowledge of the deuteron parameters till a value of $q^2 \simeq 10\ f^{-2} \simeq 0.4\ (GeV/c)^2$ but still the uncertainty of the parameters is large. The intermediate energy experiment will therefore allow also a better determination of the deuteron parameter. Since at all the energies the relevant values of t are the same (the position of the dip is constant with the energy), the same values can then be used at high energies. We think that a meaningful analysis of a high-energy pion-deuteron scattering requires a preliminary experiment at intermediate energy, in order to "calibrate" the theory. The high-energy experiment will, of course, give information about the phase of the scattering amplitude at non-zero t in an energy region which is typical of any high-energy model. It is not necessary to stress the importance of the knowledge of this quantity; as an example, we shall only remember that in the framework of a Regge pole theory, it will give a direct information about the t dependence of the Pomeranchuk (P) and the p′ trajectories.

*) It is important, however, to choose an energy far enough from a πp resonance, since near a resonance the Galuber theory shows some difficulties, connected with the rapid variation of the scattering amplitude with the energy.

As a side remark, we shall say that it is not possible to interpret the dip predicted by the previous interference theory, as the dip and the following secondary maximum which are present, at moderate energies, in the elastic $\pi^{\pm}p$ angular distribution, and which could have an effect on the elastic π-d scattering. In fact, the positions of the two dips are quite different [$|t|\simeq 0.35$ $(GeV/c)^2$ for the interference dip, $|t|\simeq 0.6$ $(GeV/c)^2$ for the dip in $\pi^{\pm}p$ scattering]. Moreover, the secondary dip, which in Eq. (1) will affect the single scattering terms, will not show up in the actual π-d distribution, since at $|t| = 0.6$ $(GeV/c)^2$ the single scattering contribution is already overwhelmed by the double scattering contribution, on which the secondary dip and maximum have negligible effect.

Let us now discuss briefly the limitations of the theory.

A first limitation is the neglect of the spin-flip effects, since in the Glauber formulation all the particles are treated as spinless. The spin-non-flip and the spin-flip amplitude being incoherent, the presence of a substantial spin-flip contribution will have the effect of reducing the deepness of an eventual dip. This difficulty can, however, be taken into account by reformulating the shadow theory with a correct treatment of the spin variables.

Another limitation comes from the fact that one always considers the deuteron as coupled only to the proton-neutron system; this effect has been analysed by Gross[7], who has found that it is small when the momentum transfer is not too high.

A third and more drastic limitation comes from the fact that in the double scattering term one neglects inelastic intermediate states.

For all these reasons, we think that a check of the theory in the intermediate energy region would be very important. In the high-energy experiment one has also the possibility of an indirect check by looking at the large-angle scattering, well after the dip and the subsequent shoulder, since there, in the Glauber theory, the magnitude of the differential cross-section depends almost on the total $\pi^{\pm}p$ cross-sections and on the deuteron parameters, while its t-dependence is a function only of the (known) slope of the $\pi^{\pm}p$ elastic differential cross-section.

2. THE EXPERIMENTAL SET-UP

The apparatus shown in Fig. 1 will allow us to measure the differential cross-section for π-d elastic scattering in a range of momentum transfer from 0.15 to 1.2 $(\mathrm{GeV}/c)^2$, for an intermediate value of the kinetic energy of the incident pion; in particular, the pion momentum has been taken to be 900 MeV/c. The experimental problems connected with the detection of the deuterons, which is the most delicate part of the experiment, are identical, however, at low and high energy. The pion branch will be different, because of the fact that at high energy the particles are much more concentrated forward, and the general background will be very different too.

In order to get an idea of the magnitude of the cross-section we want to measure, let us look at the existing p-d elastic scattering data. In the range of momentum transfer we are interested in, the cross-section does not depend very much on the kinetic energy of the incident proton[3,9,10]. The dependence of the p-d elastic scattering cross-section on the momentum transfer is shown typically in Fig. 2, for a proton kinetic energy of 2 GeV[3]. The superimposed curves are the theoretical predictions of Coleman and Franco[4], taking into account double scattering.

The angular correlation between π and d is shown in Fig. 3 for a 0.9 GeV/c incident momentum, as well as the π and p correlation in the elastic scattering on a proton at rest. In Fig. 4 the quantities relevant to the detection of deuterons are shown.

We propose to perform the low-energy experiment in the q_{3b} beam. The experimental area available at present is shown in Fig. 5. At 2.8 m from the centre of the last lens, a 7 mm diameter image is obtained, with a flux of 10^5 π^- per 3 x 10^{11} interacting protons, corresponding to a momentum bite of ± 0.5%[11]. At the image the beam has a horizontal divergency of ± 35 mrad, and a vertical divergency of ± 5 mrad.

The liquid deuterium target is the one used in the ρ-$\pi\gamma$ experiment, 3 cm diameter, 10 cm length. The total thickness in a direction normal to the beam is 0.343 g/cm^2, that is 0.37×10^{-2} rad. length (see Appendix 1). Therefore the deuterons come out of the target if the momentum transfer is larger than 0.08 (GeV/c)^2; at 0.15 (GeV/c)^2 the residual range is 0.5 g/cm^2, while the multiple scattering angle is ~ 12 mrad. The spark chambers and the path in air give a contribution to multiple scattering of the same order, but an exact calculation has still to be performed, taking into account the energy losses in the various materials, and their different weight in the track determination. The situation becomes better at higher momentum transfer; for instance, at 0.3 (GeV/c)^2 the multiple scattering is two times smaller.

The detector consists of three systems of three wire spark chambers each, with magnetostrictive read-out, plus scintillation counters, for triggering. Part of these chambers has already been built and tested in the laboratory and in a beam. Some partial description has been given[12]. The accuracy for locating a spark is 0.3 mm. The resolving power for two nearby sparks is 2 mm for the smaller chambers and 4 mm for the larger one. However, the existing readout and data acquisition system limit the resolving power to 4 mm and the accuracy of location of a spark to 0.5 mm. The efficiency of the chambers does not change when the angle between the tracks and the wire planes is increased up to values as large as 50°, while the standard error in the location of the sparks does not increase appreciably up to values of 20°~ 25°.

The reason for having three spark chambers on each ionizing branch is to allow reconstruction in space and to increase the efficiency against spurious sparks. The central chamber will be placed slightly rotated in a plane parallel to the other two in order to solve, as usual, the ambiguities when more than one spark is present.

The trigger is given by 1, $\bar{2}$, $\bar{3}$, 4, 5. The counters 1, 2, 3 have dimensions $12 \times 2 \times 0.5$ cm^3, $10 \times 10 \times 1$ cm^3 with a central window 2×0.5 cm^2, $15 \times 15 \times 1$ cm^3, respectively. The counters 4 and 4bis consist of 5 scintillator strips each, 130 cm long. The position of the counters take into account the variation of time-of-flight with the recoil angle, and the velocity of propagation of the light in the scintillator. The delay between the zero time, given by the incident particle, and the counter 4 pulse is the same for all deuterons, in the accepted solid angle. It differs by at least 6 nsec (see Fig. 6) from the time-of-flight of the recoil proton going at the same angle in the elastic π-p scattering. A time selection allows the separation of p from deuterons, already in the trigger. Furthermore, the counter 5 consists also of five strips of scintillator 50 cm long, each of them in coincidence with the corresponding strip of counter 4, so as to allow a rough check of coplanarity at the triggering stage. In order to cover the same range of azimuthal angle, the strips of counter 4 are suitably shaped.

We assume that the most important background at this energy is the pion-proton quasi-elastic scattering. Due to the smallness of the deuteron binding energy, the cross-section for the quasi-elastic scattering on a bound nucleon will be much larger than the cross-section for elastic π-d scattering in the momentum transfer region we are considering. To give an idea, the p-p[13)] and p-d[4,14)] cross-sections on which information is available, have been plotted in Fig. 7.

The precision in the measurement of the track directions will allow us to eliminate this background in the analysis. Moreover, the coplanarity requirement, and the time-of-flight selection should greatly reduce the spurious triggers. Only on the basis of time-of-flight, the tail of the Fermi momentum distribution of the proton (calculated assuming the Hulthen wave function as the correct description of the deuteron state) would cause in the trigger a signal-to-noise ratio of 1:1 if the π-p elastic cross-section is 50 times larger than that of the π-d, and if our time resolution is ± 1 nsec. When one considers the coplanarity requirement imposed to the trigger by the suitable coincidences between the corresponding strips of counters 4 and 5, this ratio becomes even better, although the exact figure has not yet been calculated.

Our system should be able to locate the dip in the π-d elastic scattering cross-section with high accuracy: the error in the momentum transfer due to the spread of momentum of the incident beam and to the errors in the measurement of the various particle trajectories is about 2%. Moreover, an accurate calibration of the apparatus can be done relatively easily, filling up the target with H_2 and measuring elastic π-p scattering: therefore we believe we can measure the absolute value of the π-d differential cross-section to a few per cent (including both statistical and systematic errors).

Assuming an average cross-section for π-d of 50 μb/sr and a solid angle of 0.3 sr we get: number of event/burst = $0.6 \times 10^5 \times 0.5 \times 10^{-4} \times 0.3 \times 0.8 \simeq 1$. Our system can be triggered about 5 times/burst, the limitation being due to the writing on a magnetic tape. Therefore, one could expect $\sim 2 \times 10^4$ events/day between 0.15 and 1.2 $(\mathrm{GeV}/c)^2$.

To analyse 5×10^4 events, 50 hours of 3800 computer time is required.

The possibility of performing the same kind of experiment on ^{4}He target is being taken into consideration, as well as using protons as incident particles.

3. READ-OUT ELECTRONICS

The read-out electronics for the magnetostrictive wire spark chambers has been intensively tested during a couple of months in the q_{3b} and q_{3a} test beams[15], and needs no modification for the experiment we are proposing.

The magnetostrictive signals, picked up by suitable coils at one end of the reading wires, are amplified and shaped giving standard 400 nsec, 2 V pulses. Since we read the x and y coordinate in nine chambers, a total of 18 amplifiers is required.

The whole information is then serialized in a set of magnetostrictive delay lines, according to Fig. 8. The delay lines have a standard equivalent length of 400 μsec, negligible jitter, and a resolution of 800 nsec.

The whole information regarding one single coordinate (one reference pulse plus the sparks) is then contained in a time interval of 400 μsec; the control unit, essentially a sophisticated stop scaler driven by the timing unit (one single delay line with recirculation), then starts and stops a number of successive scalers equal to the number of sparks. In other words, we do not assign "a priori" a fixed number of scalers per electrode, but only the total number of sparks we expect to have.

In the present proposal the number of sparks we expect to have is 18; with a set of 30 scalers we will then allow the occurence, for instance, of one extra track in a telescope and a total of six spurious sparks anywhere in the system.

Two 24-bit indicators, mounted as standard CERN scalers, give the number of sparks recorded for each coordinate. The display of these registers gives an immediate check-up of eventual failures in the system.

The whole writing process requires less than 8 msec; about 40 msec are then needed to record the contents of the scalers on an IBM 7330 magnetic tape unit, using standard CERN interface.

APPENDIX I

MATERIALS ON THE DEUTERON PATH

	g/cm^2		units of rad. length
Target (existing)	0.2610	D_2	22.50×10^{-4}
	0.0187	mylar *) (target wall)	4.57 "
	0.0270	Al heat shield	1.13 "
	0.0014	mylar aluminized	0.34 "
	0.0347	mylar vacuum	8.48 "
Spark chambers walls	0.056	mylar (6 × 0.009)	14.00 "
wire **)	0.1068	Cu	78.00 "
Air path (over 1.5 m)	0.2	air	59.00 "

*) 62.5% C; 33.3% O; 4.2% H.

**) The wire is 0.1 mm diameter Cu, the interspace is 1 mm. For 12 wire planes, the average thickness traversed by one particle is 0.12 mm.

REFERENCES

1) V. Franco, Phys.Rev.Letters 16, 944 (1966).
E. Coleman, Michigan University Thesis, July, 1966.

2) V. Franco and R.J. Glauber, Phys.Rev. 142, 1195 (1966).

3) E. Coleman, R.M. Heinz, O.E. Overseth and D.E Pellett, Phys.Rev. Letters 16, 761 (1966).

4) V. Franco and E. Coleman, Phys.Rev.Letters 17, 827 (1966).

5) H. Palevsky, in Int.Conf. on Nuclear Physics, Gatlinburg (1966).

6) W. Czyz and L. Lesniak, Physics Letters 24 B, 227 (1967).
R.H. Bassel and C. Wilkin, BNL 11274, March 1967.

7) F. Gross, Phys.Rev. 134 B, 405 (1964); 140 B, 410 (1965).
E.S. Abers, H. Burkhardt, V.L. Teplitz and C. Wilkin, Nuovo Cimento 42, 365 (1966).
L. Bertocchi and A. Capella, Nuovo Cimento (to be published).

8) M. Gourdin, M. Le Bellac, F.M. Renard and J. Tran Thanh Van, Nuovo Cimento 37, 524 (1964).
Y. Renard and J. Tran Thanh Van, Orsay preprint TH/166, Sept. 1966.

9) M.G. Meshcheriakov et al., in Proc.Int.Symposium, CERN (1956), p. 125.

10) A.V. Crewe, B. Ledley, E. Lillethun, S. Marcowitz and L.G. Pondrom, Phys.Rev. 114, 1361 (1959).

11) G. Petrucci (private communication).

12) F. Bradamante and F. Sauli, INFN/AE-66/2, 1966.
M. Renevey, CERN NP Int.Rep. 66-6 (1966).
F. Bradamante and F. Sauli, Magnetostrictive thin-gap wire spark chambers of large dimensions, May 1967, (Submitted to Nucl.Instr. Meths.); see also CERN NP Int.Rep. 66-8 (1966).

13) B. Cork, W.A. Wenzel and Ch.W. Causey, Phys.Rev. 107, 859 (1967).

14) L.S. Zolin et al., JETP Letters 3, 8 (1966).

15) F. Bradamante and F. Sauli, INFN/AE-67/4, 1967.

Figure Captions

Fig. 1 : Experimental set-up, as seen in the horizontal plane. $S_1 \ldots S_9$ are two gaps wire spark chambers with magnetostrictive read-out, $C_1 \ldots C_5$ are scintillation counters.

Fig. 2 : [From V. Franco and E. Coleman, Phys.Rev. Letters 17, 827 (1966)]. Differential cross-sections in the lab system for elastic pd scattering at 2.0 GeV. The solid (broken) curve is the theoretical prediction, using nucleon-nucleon data, when double scattering is treated (neglected). The dotted curve is calculated with the experimental lower limits for α_{pn} and α_{pp}, and the dot-dashed with theoretical predictions for α_{pn} and α_{pp}; they both include double scattering.

Fig. 3 : Angular correlation between pion and deuteron (proton) for elastic pion-deuteron (proton) scattering at an incident pion momentum of 900 MeV/c. The momentum transfer (-t) of the deuteron is also shown, as a function of the deuteron scattering angle.

Fig. 4 : Momentum transfer (kinetic energy), range in deuterium, and multiple scattering angle for unit of radiation length, vs. deuteron momentum.

Fig. 5 : q_{3b} beam layout at C.P.S.

Fig. 6 : Deuteron (proton) time-of-flight per metre and range in carbon as a function of deuteron (proton) scattering angle in pion-deuteron (-proton) elastic scattering at 900 MeV/c.

Fig. 7 : Differential cross-section in the laboratory as a function of the solid angle of the recoil particle in p-d and p-p elastic scattering at 2 GeV.

Fig. 8 : Block diagram for the read-out electronics.

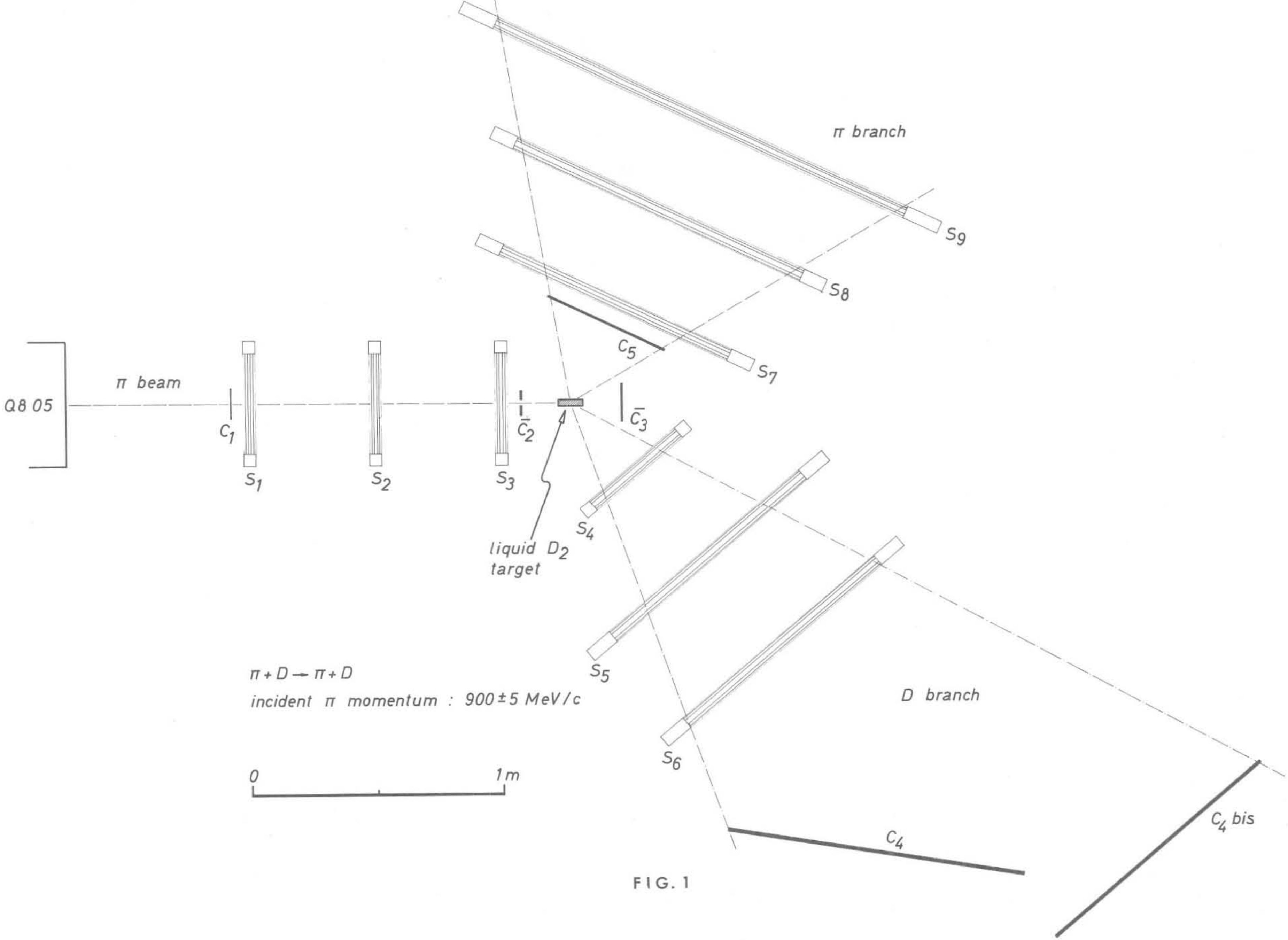
π branch
S9
S8
S7
C5
Q8 05
π beam
C1
S1
S2
S3
C̄2
C̄3
S4
liquid D2
target
S5
S6
π + D → π + D
incident π momentum : 900 ± 5 MeV/c
D branch
0
1m
C4
C4 bis

FIG. 1

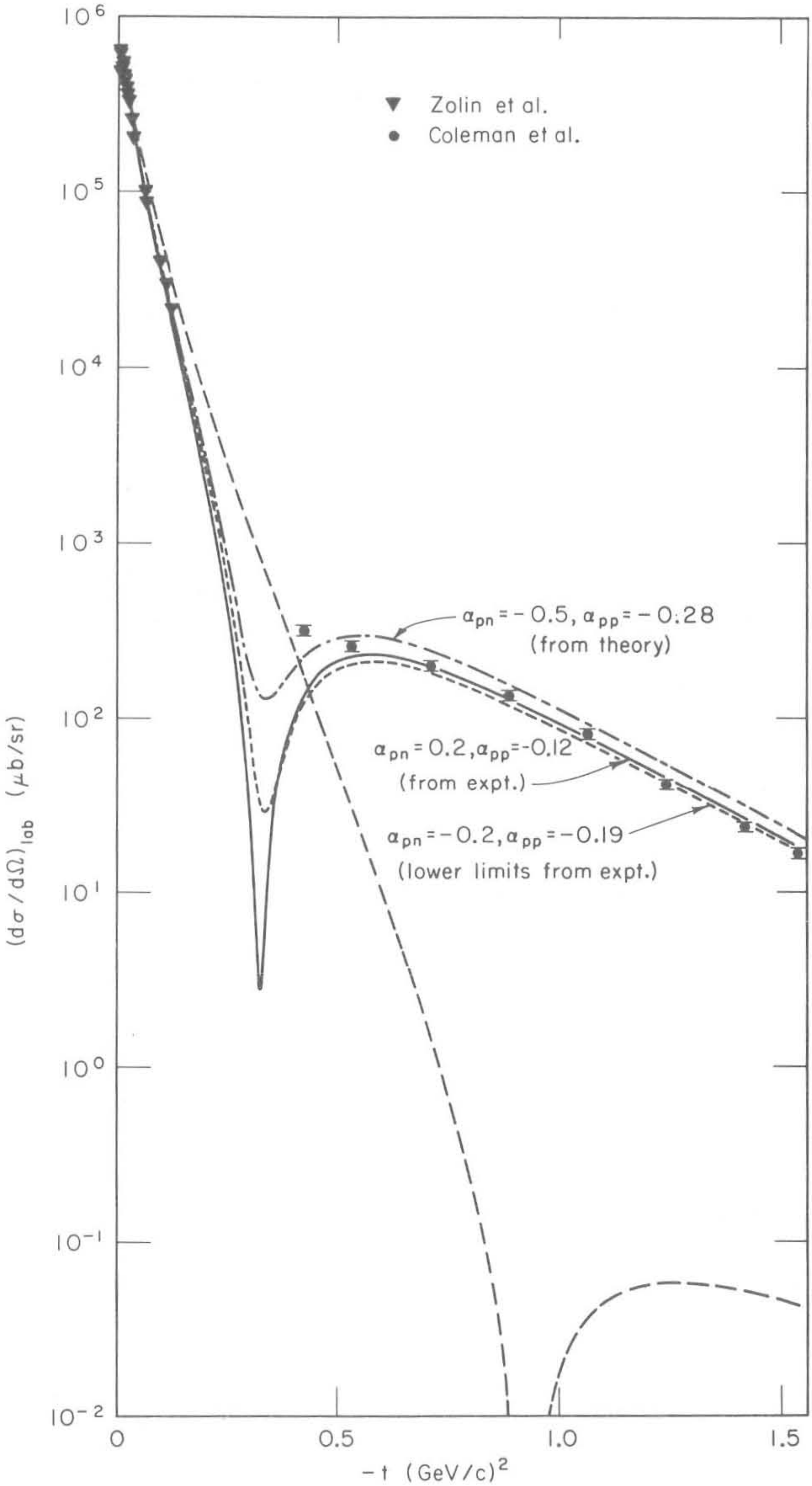

Zolin et al.
Coleman et al.
$\alpha_{pn} = -0.5, \alpha_{pp} = -0.28$
(from theory)
$\alpha_{pn} = 0.2, \alpha_{pp} = -0.12$
(from expt.)
$\alpha_{pn} = -0.2, \alpha_{pp} = -0.19$
(lower limits from expt.)
$(d\sigma/d\Omega)_{lab}$ (μb/sr)
$-t$ (GeV/c)^2

FIG. 2

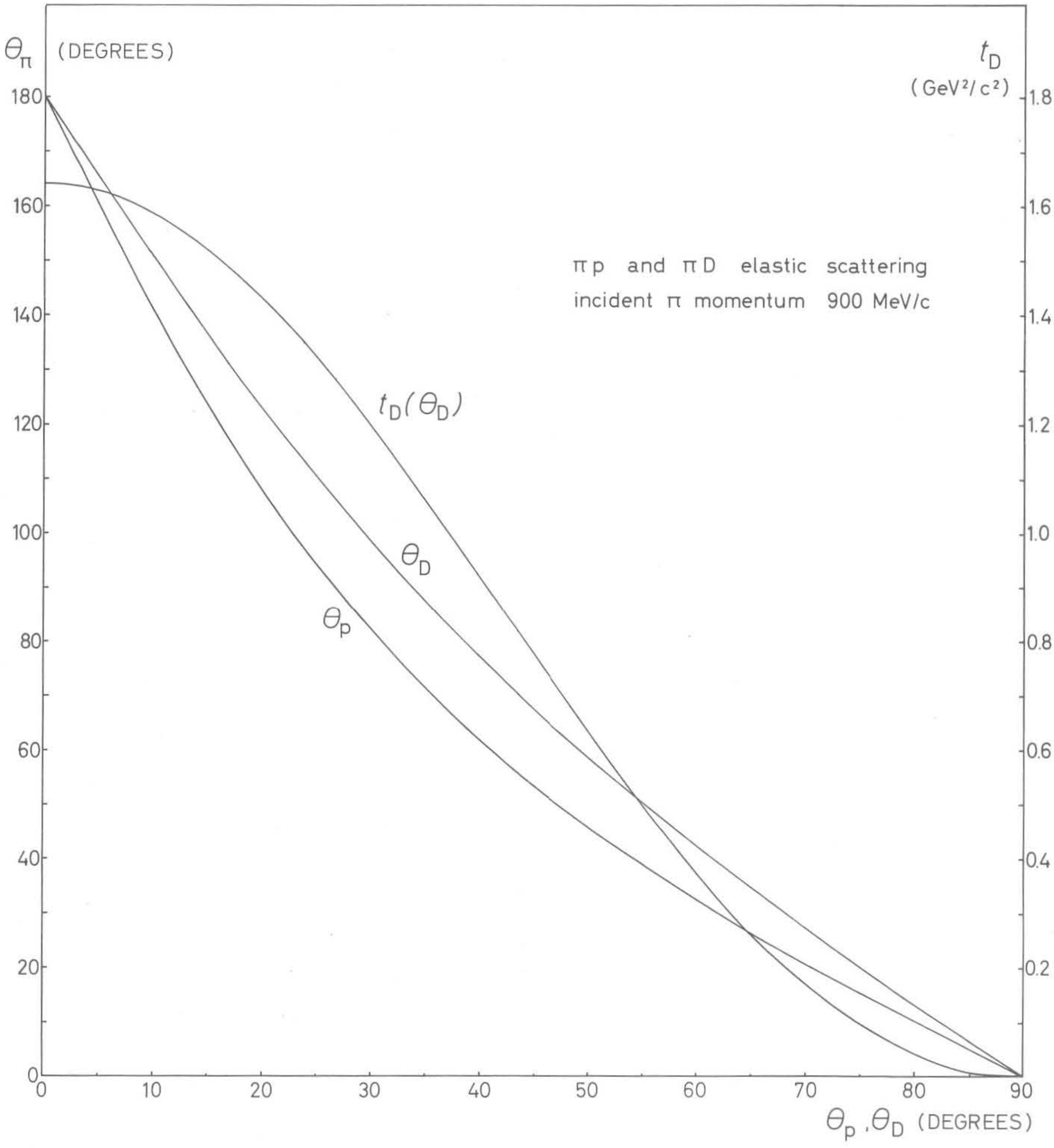

θ_π (DEGREES)
t_D
(GeV^2/c^2)
180
160
140
120
100
80
60
40
20
0
1.8
1.6
1.4
1.2
1.0
0.8
0.6
0.4
0.2
πp and πD elastic scattering
incident π momentum 900 MeV/c
$t_D(\theta_D)$
θ_D
θ_p
0
10
20
30
40
50
60
70
80
90
θ_p, θ_D (DEGREES)

FIG.3

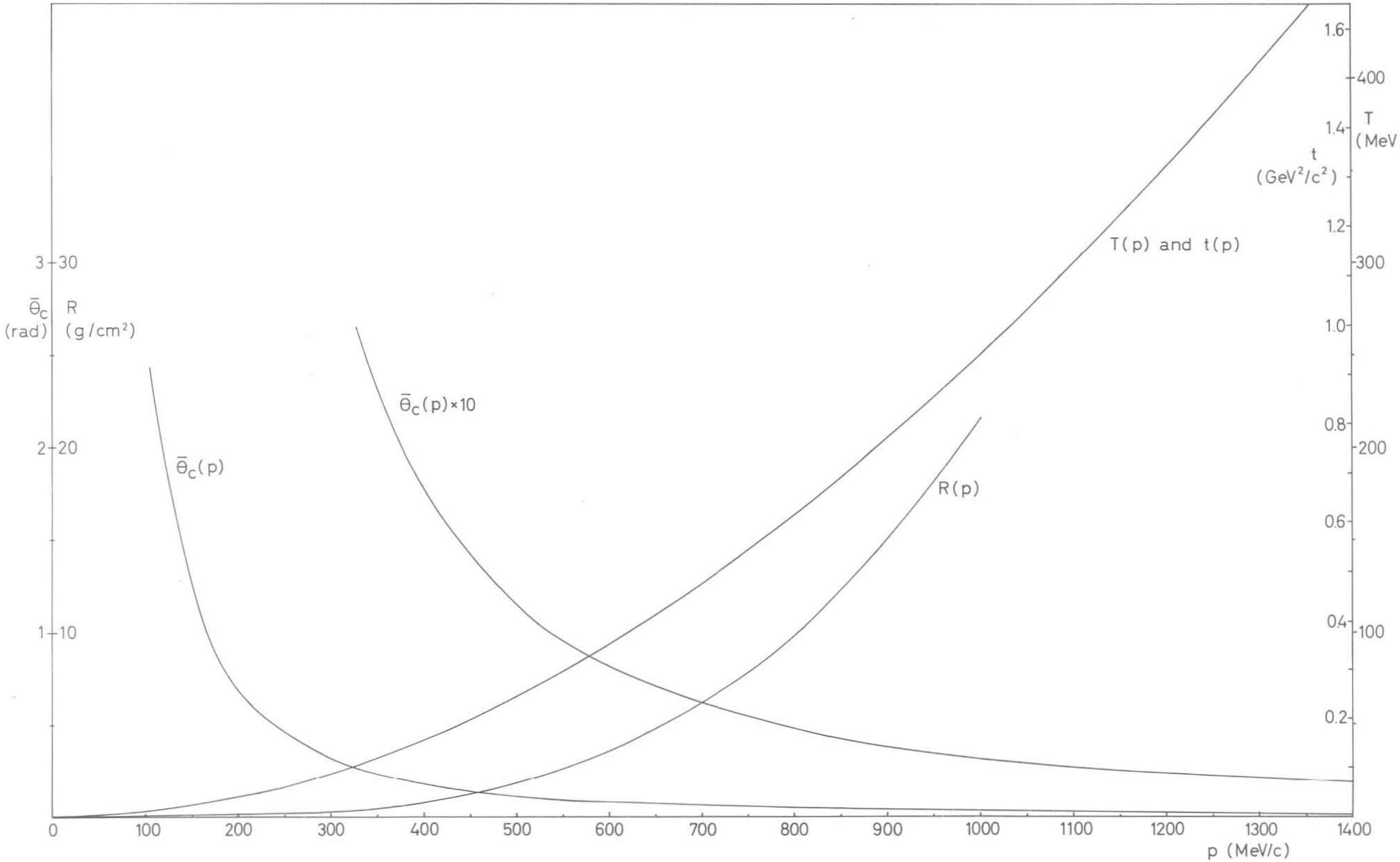

$\bar{\theta}_c$ (rad)
R (g/cm²)
3 30
2 20
1 10
$\bar{\theta}_c(p)$
$\bar{\theta}_c(p)\times 10$
R(p)
T(p) and t(p)
t (GeV²/c²)
T (MeV)
1.6
1.4
1.2
1.0
0.8
0.6
0.4
0.2
400
300
200
100
0 100 200 300 400 500 600 700 800 900 1000 1100 1200 1300 1400
p (MeV/c)

FIG. 4

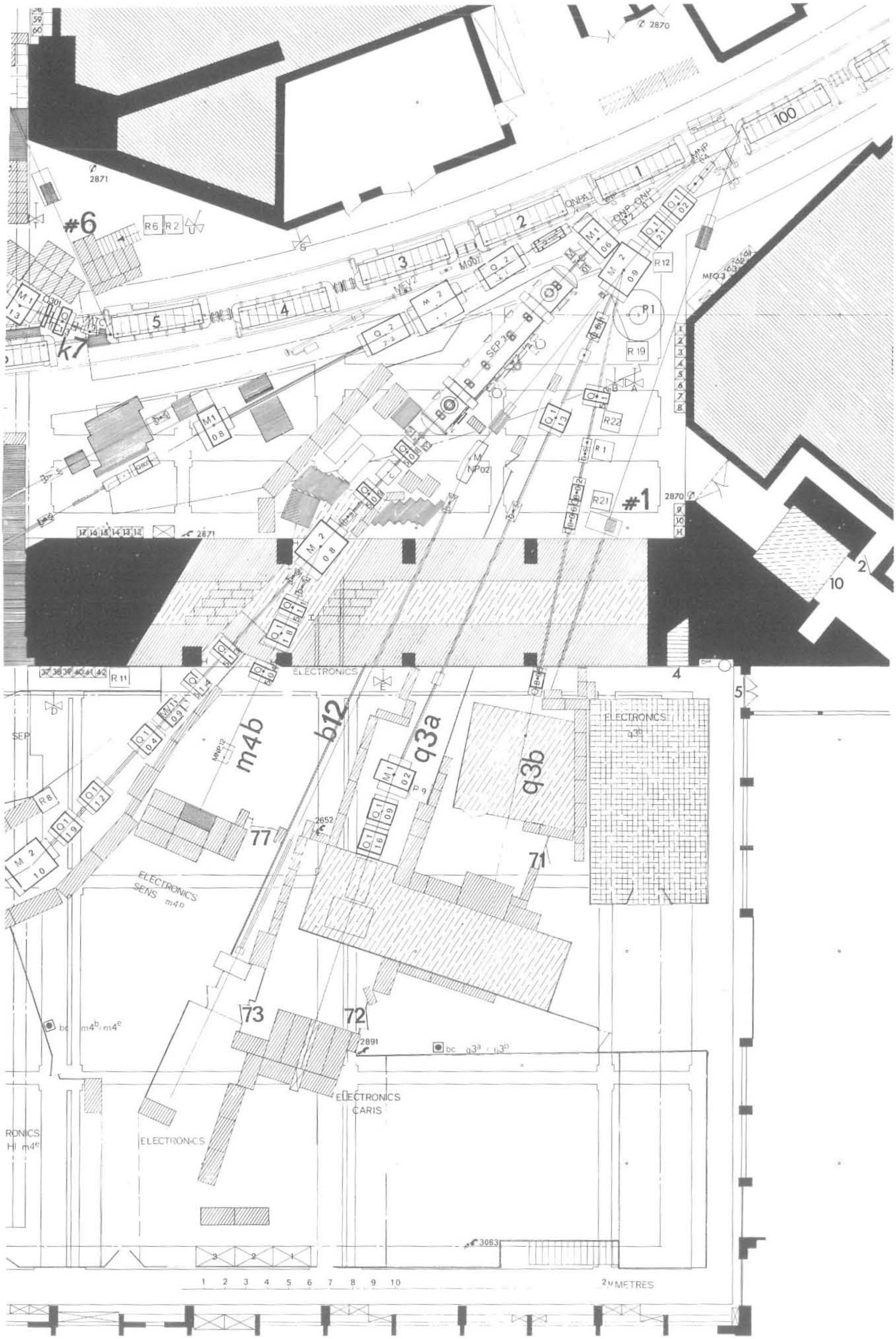
#6
#1
k7
SEP 3
ELECTRONICS
m4b
b12
q3a
q3b
77
71
73
72
ELECTRONICS SENS m4b
ELECTRONICS CARIS
ELECTRONICS
20 METRES

FIG. 5

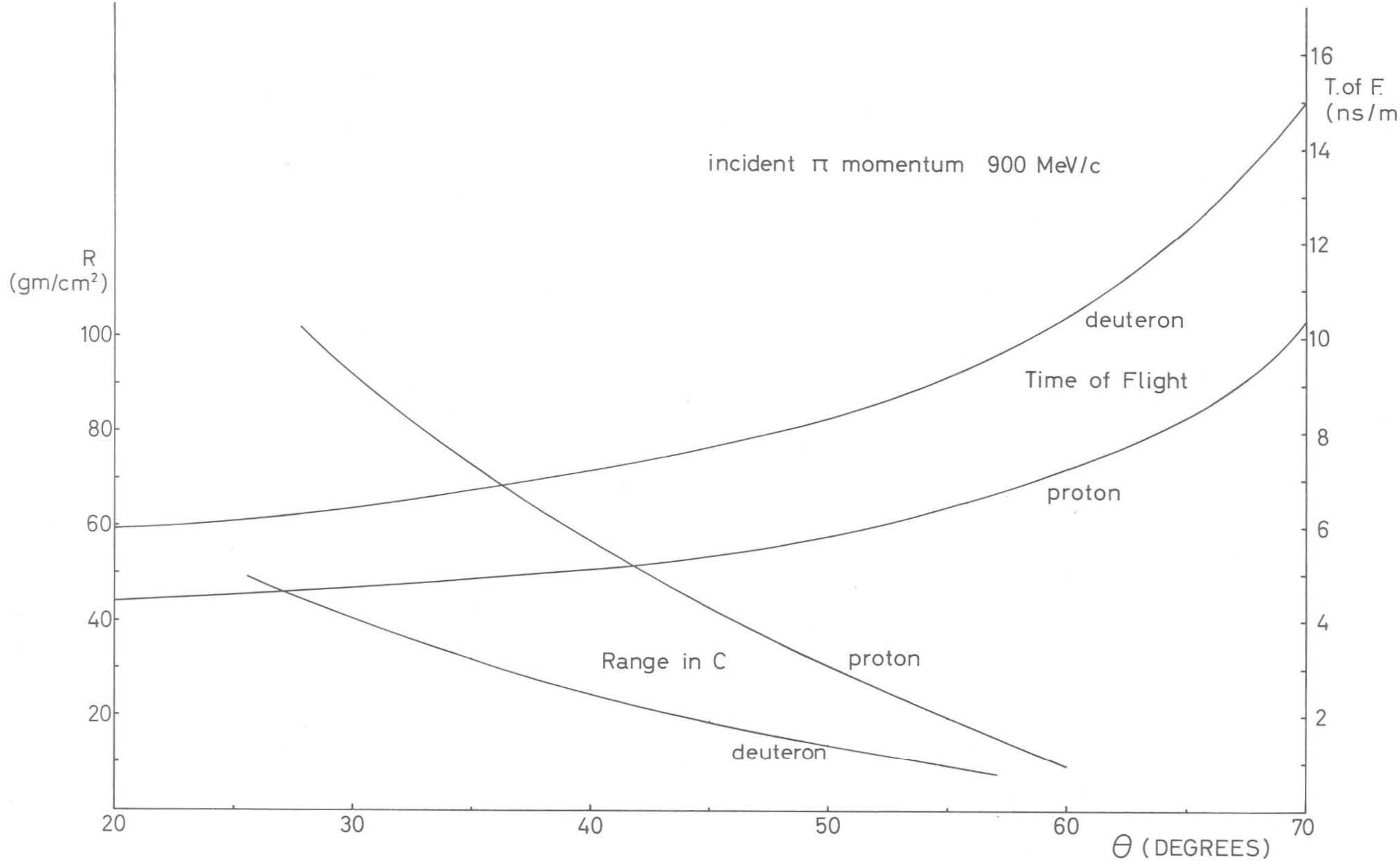

R
(gm/cm²)
100
80
60
40
20
20
30
40
50
60
70
θ (DEGREES)
16
T. of F.
(ns/m)
14
12
10
8
6
4
2
incident π momentum 900 MeV/c
deuteron
Time of Flight
proton
Range in C
proton
deuteron

FIG. 6

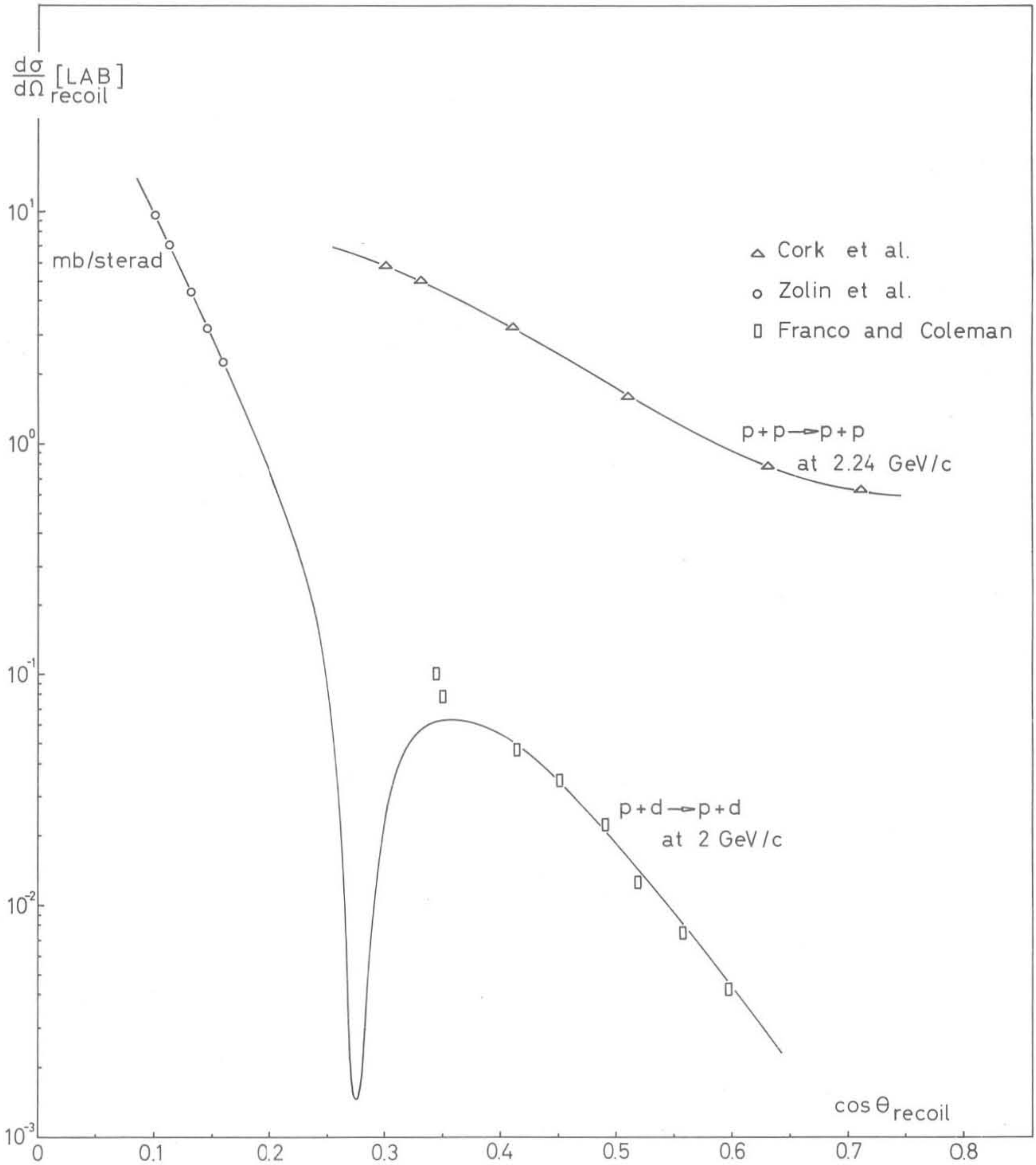

$\frac{d\sigma}{d\Omega}$ [LAB] recoil
mb/sterad
10^1
10^0
10^{-1}
10^{-2}
10^{-3}
Cork et al.
Zolin et al.
Franco and Coleman
p+p → p+p at 2.24 GeV/c
p+d → p+d at 2 GeV/c
cos θ recoil
0
0.1
0.2
0.3
0.4
0.5
0.6
0.7
0.8

FIG. 7

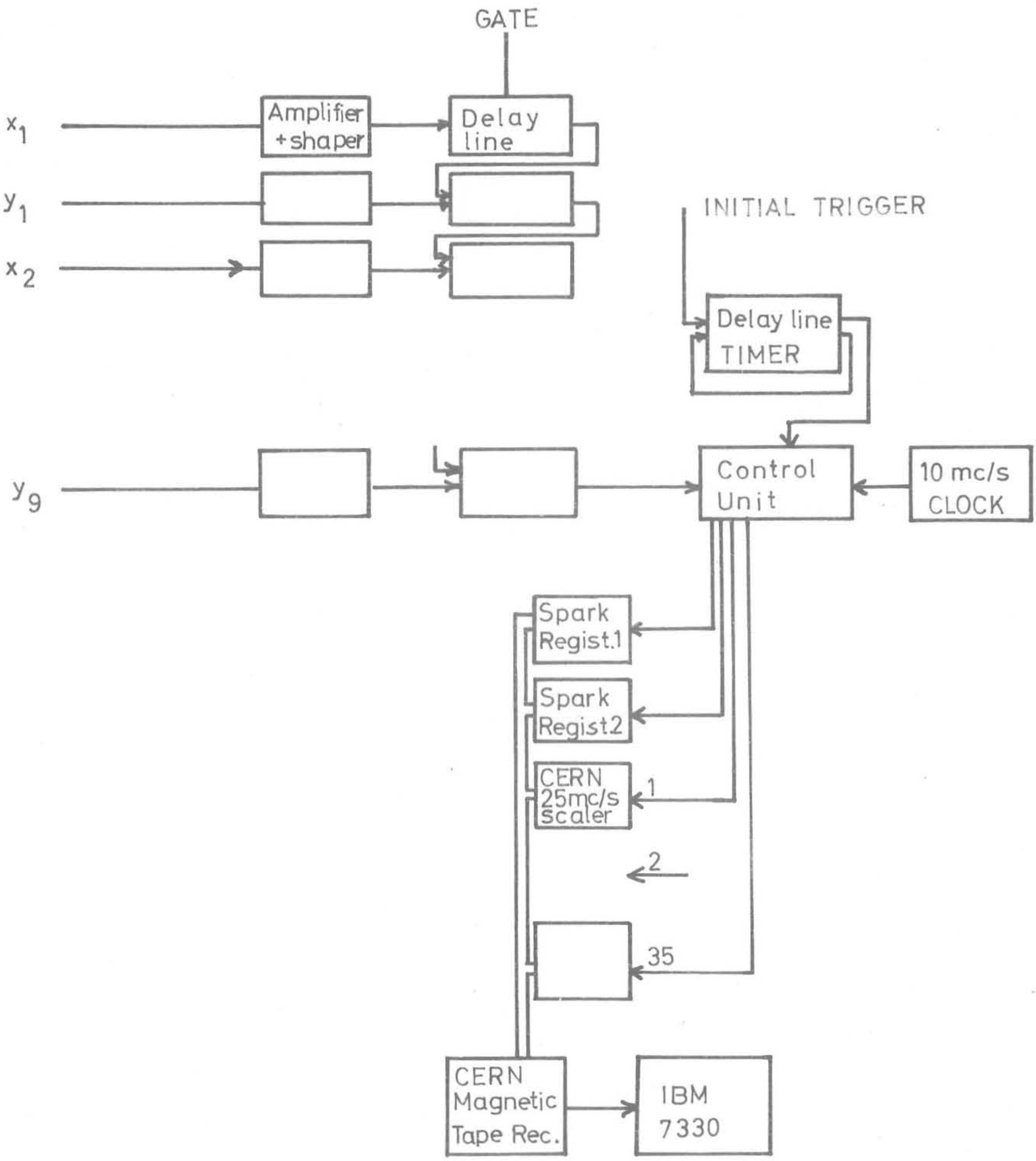

GATE
x1
y1
x2
y9
Amplifier
+shaper
Delay
line
INITIAL TRIGGER
Delay line
TIMER
Control
Unit
10 mc/s
CLOCK
Spark
Regist.1
Spark
Regist.2
CERN
25mc/s
scaler
1
2
35
CERN
Magnetic
Tape Rec.
IBM
7330

FIG. 8